

Weak spin interactions in Mott insulating $\text{La}_2\text{O}_2\text{Fe}_2\text{OSe}_2$

E. E. McCabe,^{1,2,*} C. Stock,³ E. E. Rodriguez,⁴ A. S. Wills,⁵ J. W. Taylor,⁶ and J. S. O. Evans^{1,†}

¹*Department of Chemistry, Durham University, Durham DH1 3LE, United Kingdom*

²*School of Physical Sciences, University of Kent, Canterbury CT2 7NH, United Kingdom*

³*School of Physics and Astronomy, University of Edinburgh, Edinburgh EH9 3JZ, United Kingdom*

⁴*Department of Chemistry and Biochemistry, University of Maryland, College Park, Maryland 20742, USA*

⁵*Department of Chemistry, University College London, 20 Gordon Street, London WC1H 0AJ, United Kingdom*

⁶*ISIS Facility, Rutherford Appleton Laboratory, Chilton, Didcot OX11 0QX, United Kingdom*

(Received 3 September 2013; published 10 March 2014)

Identifying and characterizing the parent phases of iron-based superconductors is an important step towards understanding the mechanism for their high-temperature superconductivity. We present an investigation into the magnetic interactions in the Mott insulator $\text{La}_2\text{O}_2\text{Fe}_2\text{OSe}_2$. This iron oxyselenide adopts a 2- k magnetic structure with low levels of magnetic frustration. This magnetic ground state is found to be dominated by next-nearest-neighbor interactions J_2 and J_2' and the magnetocrystalline anisotropy of the Fe^{2+} site, leading to 2D-Ising-like spin $S = 2$ fluctuations. In contrast to calculations, the values are small and confine the spin excitations below ~ 25 meV. This is further corroborated by sum rules of neutron scattering. This indicates that superconductivity in related materials may derive from a weakly coupled and unfrustrated magnetic structure.

DOI: [10.1103/PhysRevB.89.100402](https://doi.org/10.1103/PhysRevB.89.100402)

PACS number(s): 74.70.Xa, 75.25.-j

The discovery of iron-based superconductivity at high temperatures in pnictide [1] and chalcogenide [2] systems highlights the importance of magnetism in high- T_c superconductivity [3]. Despite the similar phase diagrams and the proximity of magnetism to superconductivity reported for both the cuprate and iron-based superconductors, these materials otherwise seem remarkably different: the cuprate systems are based on doping a strongly correlated Mott insulating state [4], while the parent phases for the iron-based materials are either metallic, semiconducting, or semimetallic [5–7]. However, recent work has revealed electron correlation effects in iron pnictides suggesting that the iron-based systems may be close to the Mott boundary, yet a strongly correlated parent compound has not been clearly identified for chalcogenide and pnictide superconductors [8,9]. Also, the spin state of the Fe^{2+} in these systems is not understood with different theories suggesting $S = 1$ or 2 ground states [10–12]. In this Rapid Communication, we investigate the magnetic interactions in the Mott insulating iron oxyselenide $\text{La}_2\text{O}_2\text{Fe}_2\text{OSe}_2$.

This layered material [Fig. 1(a)] adopts a tetragonal crystal structure composed of fluorite-like $[\text{La}_2\text{O}_2]^{2+}$ layers and $[\text{Fe}_2\text{O}]^{2+}$ sheets that are separated by Se^{2-} anions. The $[\text{Fe}_2\text{O}]^{2+}$ sheets adopt an unusual anti- CuO_2 arrangement with Fe^{2+} cations coordinated by two in-plane oxygens and four Se^{2-} anions above and below the plane, leading to layers of face-shared FeO_2Se_4 trans octahedra [13]. The Fe grid is similar to that in LaFeAsO and FeSe , has similar $\sim 90^\circ$ Fe-Se-Fe interactions but contains additional in-plane O^{2-} ions.

$\text{La}_2\text{O}_2\text{Fe}_2\text{OSe}_2$ has been described as a Mott insulator and theoretical work suggests that it is more strongly correlated than LaFeAsO [14]. $\text{La}_2\text{O}_2\text{Fe}_2\text{OSe}_2$ orders antiferromagnetically (AFM) below ~ 90 K [15] and two magnetic structures have been discussed for the $[\text{Fe}_2\text{O}]^{2+}$ layers: a collinear model [Fig. 1(b)] similar to that reported for Fe_{1+x}Te [16,17] and

the 2- k model [Fig. 1(c)] first proposed for $\text{Nd}_2\text{O}_2\text{Fe}_2\text{OSe}_2$ [18]. These two models are indistinguishable from powder diffraction work and in the absence of single crystals of sufficient size and quality, this ambiguity has not been

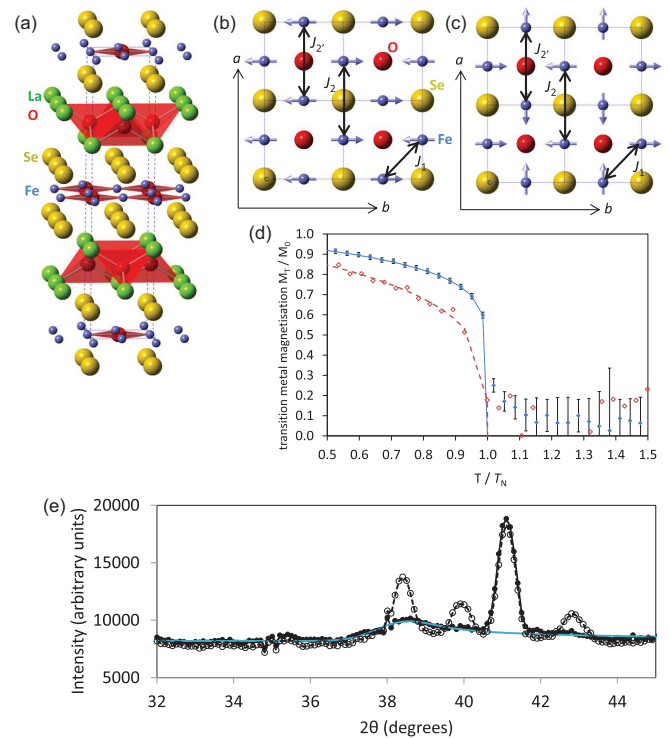


FIG. 1. (Color online) (a) Nuclear cell of $\text{La}_2\text{O}_2\text{Fe}_2\text{OSe}_2$, (b) collinear model, and (c) 2- k model with the three intraplanar exchange interactions J_1 , J_2 and J_2' shown. (d) Evolution of magnetic moment for $\text{La}_2\text{O}_2\text{Fe}_2\text{OSe}_2$ and $\text{La}_2\text{O}_2\text{Mn}_2\text{OSe}_2$ (Ref. [27]) with $M_{0\text{Fe}} = 3.701(8) \mu_B$, $T_N = 89.50(3)$ K, and $\beta_{\text{Fe}} = 0.122(1)$; $M_{0\text{Mn}} = 4.5(2) \mu_B$, $T_N = 168.1(1)$ K, and $\beta_{\text{Mn}} = 0.24(3)$. (e) Narrow 2θ range of raw NPD data for $\text{La}_2\text{O}_2\text{Fe}_2\text{OSe}_2$ collected at 91.2 K and at 88.2 K; the Warren-type peak is shown by the solid blue line.

*e.e.mccabe@kent.ac.uk

†john.evans@durham.ac.uk

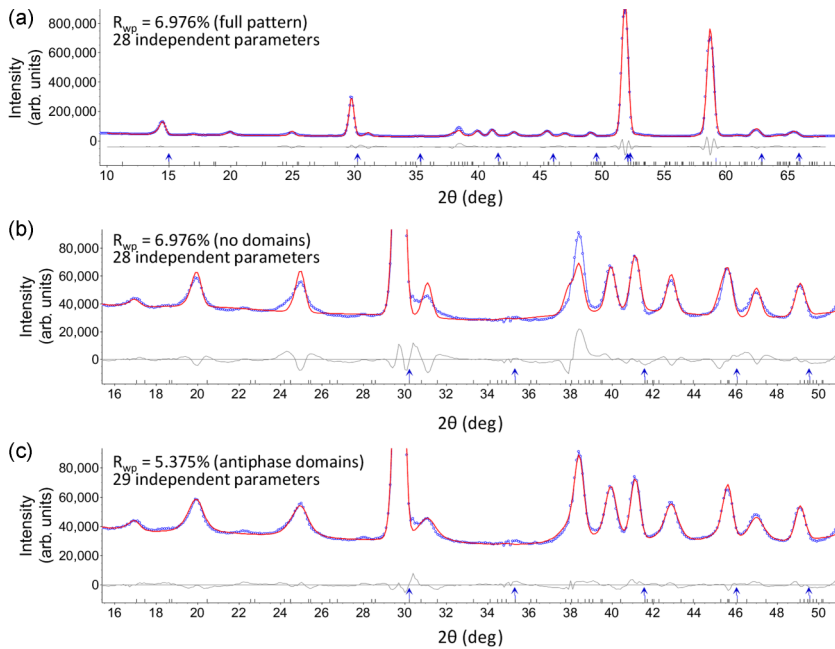


FIG. 2. (Color online) Rietveld refinements (D20, $\lambda = 2.41 \text{ \AA}$) with the $2\text{-}k$ model showing (a) wide 2θ range with both nuclear (blue arrows) and magnetic (black tick marks) phases; (b) refinement with the *same* peak shape for both nuclear and magnetic phases; (c) refinement including antiphase boundaries in the magnetic phase. Observed and calculated (upper) and difference (lower, at zero intensity) profiles are shown by blue points, red, and gray lines, respectively. The tick marks do not include a refined zero offset of $\sim 0.4^\circ$.

resolved. We present experimental results here that favor the $2\text{-}k$ model proposed by Fuwa *et al.* [18] and hope to resolve this ambiguity.

The related pnictide and chalcogenide parent compounds have been the subject of theoretical and experimental studies. Analogous to the cuprates, the spin exchange constants and spin-wave dispersions in these parent compounds are large, extending up to energy transfers of ~ 100 meV, reflecting strong Fe-Fe coupling [19–24]. Electronic structure calculations for $\text{La}_2\text{O}_2\text{Fe}_2\text{OSe}_2$ suggest similar exchange constants to the pnictides but with considerable electronic band narrowing [14]. Until now, neutron inelastic measurements to corroborate such predictions have not been reported for $\text{La}_2\text{O}_2\text{Fe}_2\text{OSe}_2$. We present a combined study of the magnetic structure and fluctuations to understand the interactions in $\text{La}_2\text{O}_2\text{Fe}_2\text{OSe}_2$ using neutron powder diffraction (NPD) and inelastic measurements. Full experimental details are provided in the Supplemental Material [25].

We first discuss the elastic magnetic scattering near T_N (~ 89 K) [Fig. 1(e)]. A broad, low-intensity, asymmetric Warren-like peak develops between 103 and 91 K centered at $\sim 37^\circ 2\theta$, characteristic of 2D short-ranged ordering [26]. Fitting with a Warren function gives a 2D correlation length of $\sim 23 \text{ \AA}$ at 103 K that increases to $\sim 90 \text{ \AA}$ (about 20 times the in-plane cell parameter) just above T_N . Below T_N , magnetic Bragg reflections appear with the most intense peak at $2\theta \sim 38^\circ$, such that any remaining diffuse scatter becomes hard to fit.

Magnetic Bragg reflections appear below T_N , to which the $2\text{-}k$ (Fig. 2) and collinear spin models give indistinguishable fits. In contrast to the report on $\text{Sr}_2\text{F}_2\text{Fe}_2\text{OS}_2$, there is no difference in the magnitude of Fe moments for these two models [28]. The magnetic Bragg reflections observed for $\text{La}_2\text{O}_2\text{Fe}_2\text{OSe}_2$ are anisotropically broadened similarly to $\text{Sr}_2\text{F}_2\text{Fe}_2\text{OS}_2$, suggesting that both have similar magnetic microstructures. This peak broadening can be described by an expression for antiphase boundaries perpendicular to the c axis [29] [Fig. 2(c)] with a magnetic correlation length $\xi_c(T =$

$2 \text{ K}) = 45(3) \text{ \AA}$ that is essentially independent of temperature [$\xi_c(T = 88 \text{ K}) = 42(6) \text{ \AA}$]. No such peak broadening has been reported for the Mn^{2+} and Co^{2+} analogs [27,30,31].

Sequential NPD Rietveld refinements indicate a smooth increase in the ordered Fe^{2+} moment on cooling. This magnetic order parameter is shown in Fig. 1(d) with critical exponent $\beta_{\text{Fe}} = 0.122(1)$, similar to the 2D-Ising-like behavior of $\text{La}_2\text{O}_2\text{Co}_2\text{OSe}_2$ and BaFe_2As_2 [31,32]. This is in contrast to the Mn analog with an exponent $\beta = 0.24(3)$ [Fig. 1(d)] reflecting greater 3D-like character [27]. The ordered Fe^{2+} moment in $\text{La}_2\text{O}_2\text{Fe}_2\text{OSe}_2$ determined from our Rietveld refinements [$3.50(5) \mu_B$ at 2 K] is larger than that reported previously ($\sim 2.8 \mu_B$) [15,33], due to improved fitting of magnetic Bragg peaks [Fig. 2(c)]; our value is similar to that reported for $\text{Sr}_2\text{F}_2\text{Fe}_2\text{OS}_2$ [$3.3(1) \mu_B$] [28] and in the parent phase of superconducting $\text{K}_x\text{Fe}_{2-y}\text{Se}_2$ ($3.3 \mu_B$) [34,35].

We now discuss spin excitations characterizing the magnetic interactions shown in Fig. 1. Figure 3 shows the temperature-dependent, powder-averaged inelastic response. The spectra at 2 K show the magnetic response is gapped and localized in momentum [Fig. 3(a)] and softens on warming [Fig. 3(b)] until gapless scattering is observed for $T > T_N$ [Fig. 3(c)]. This is further illustrated in Figs. 3(d) and 3(e) (showing Q -integrated energy scans) and in lower resolution scans shown in Figs. 3(f) and 3(g). The intensity distribution at the gap edge is sensitive to the dimensionality of the interactions and can be quantified through use of the first moment sum rule. Figure 3(d) shows a comparison of the momentum-integrated intensity with calculations based on the single-mode approximation for an isotropic dispersion in a one-dimensional (1D) chain, 2D plane, or 3D structure [36–38]. The 2D model gives the best description consistent with the 2D-Ising critical properties discussed above.

Scans that probe larger energy transfers are shown in Figs. 3(f)–3(h). Surprisingly, the magnetic excitations extend up to only ~ 25 meV. This small band accounts for all of the expected spectral weight, confirmed by integrating

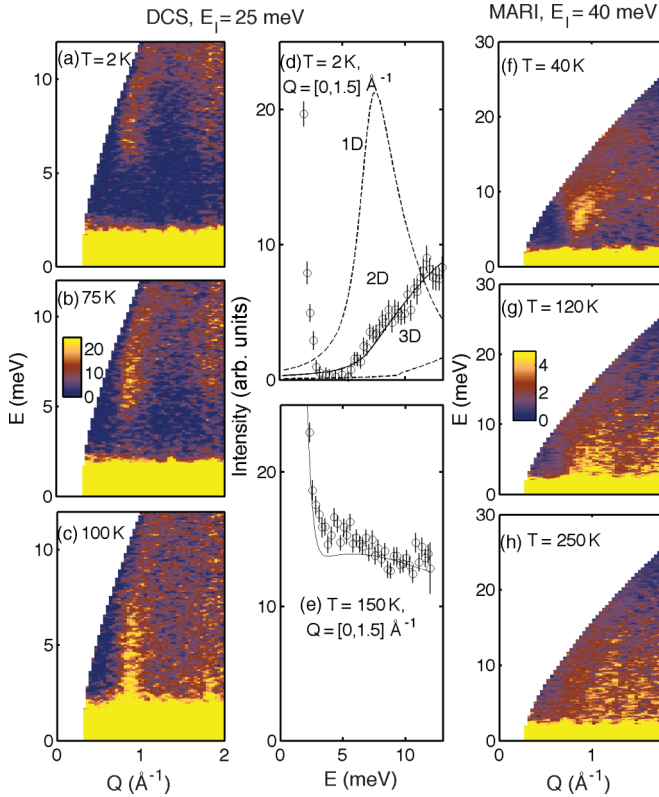


FIG. 3. (Color online) (a)–(c) Powder-averaged spectra measured on DCS. (d) Momentum-integrated energy scan at 2 K (upper) and 150 K (lower); the curves are calculations using a single-mode analysis with a 1D model, a 2D model, and a 3D model. (f)–(h) Plots of the powder-averaged temperature spectra taken on the MARI spectrometer.

the intensity and comparing with the zeroth sum rule [$\tilde{I} = \int d^2 Q \int dE S(\vec{Q}, E) / \int d^3 Q = S(S+1)$]. Our inelastic data [over energy ranges shown in Fig. 3(e)] give $\tilde{I}_{\text{inelastic}} = 3.2(4)$ for the dynamic response. The elastic magnetic moment of $3.5 \mu_B$ (determined from NPD discussed above) implies an elastic contribution to the above integral of $\tilde{I}_{\text{static}} = 2.7(1)$, giving $\tilde{I} = 5.9(4)$, close to the $S = 2$ value of 6. Over this narrow energy range, all magnetic spectral weight is accounted for.

This analysis demonstrates that the total bandwidth of the spin excitations is only ~ 20 meV. This is remarkably small when compared with Mott insulating La_2CuO_4 and $\text{YBa}_2\text{Cu}_3\text{O}_{6+x}$ (with a bandwidth of over 300 meV) and with the parent phases of the pnictides (the top of the band in BaFe_2As_2 is ~ 100 meV and ~ 150 meV in CaFe_2As_2) or the chalcogenide Fe_{1+x}Te (where excitations extend up to ~ 150 – 200 meV) [19–21,23,24]. The small bandwidth observed for $\text{La}_2\text{O}_2\text{Fe}_2\text{OSe}_2$ implies that magnetic exchange interactions are about an order of magnitude smaller than in the cuprates and pnictides.

To estimate these exchanges, calculations were performed fixing the moment direction with a single-ion anisotropy and considering Heisenberg spin exchange. The calculation is sensitive to the signs of the interactions and the ground state. These calculations were carried out based on both the collinear and 2- k magnetic ground states (Fig. 1) and results are

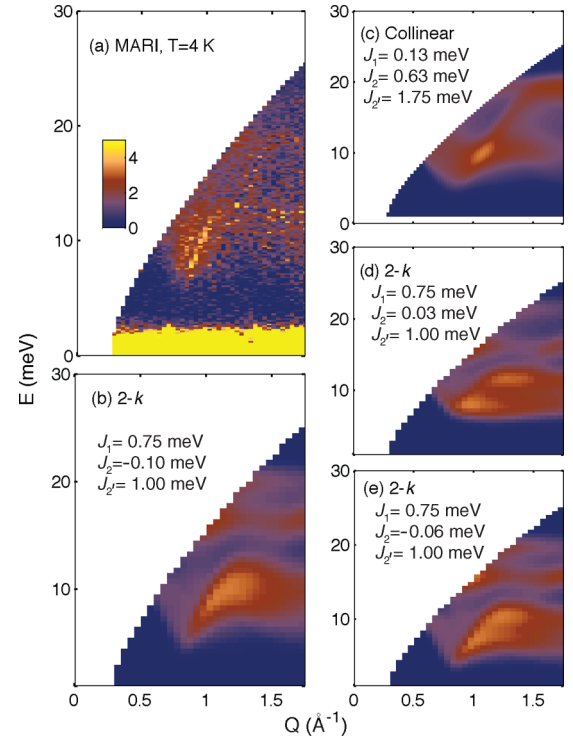


FIG. 4. (Color online) (a) MARI scans with $E_i = 40$ meV and spin-wave models for (b) the 2- k structure and (c) the collinear magnetic structure. (d) and (e) Effect of weak AFM and FM values of the J_2 exchange interaction on simulated spectra.

shown in Fig. 4. The experimental spectrum can be reproduced reasonably well for the 2- k ground state with $J_1 = 0.75$ meV, $J_2 = -0.10$ meV, and $J_2' = 1.00$ meV [Fig. 4(b)] and for the collinear ground state with $J_1 = 0.13$ meV, $J_2 = 0.63$ meV, and $J_2' = 1.00$ meV [Fig. 4(c)]. The predicted Θ_{CW} , to be compared with a $T_N \sim 90$ K, are ~ 110 K for the 2- k and ~ 75 K for the collinear models. These two models give comparable descriptions of the data and differ mainly in the sign of the J_2' interaction with the 2- k (collinear) ground state giving a FM (AFM) value.

We now compare the collinear and 2- k models. The collinear model [Fig. 1(b)] is a single- k model with $\vec{k} = (0 \frac{1}{2} \frac{1}{2})$. This k vector splits the moments of the Fe site ($4c$ site in $I4/mmm$) into two orbits that order under separate irreducible representations (irreps) with the moments along the b axis. The irreps and basis vectors involved are labeled $N_2^+(B_{3g})$ and $N_1^-(B_{2g})$ according to ISODISTORT [39], and $\Gamma_2\psi_1$ and $\Gamma_3\psi_2$ following SARAh [40]. In terms of energy, none of the three intraplanar exchange interactions are satisfied in the collinear structure, making it disfavored on energetic grounds. As the mean fields experienced by the different orbits are orthogonal, they would order separately and so this model would also be disfavored on entropic arguments.

The 2- k model [Fig. 1(c)] can, to a first approximation, be described by the spin Hamiltonian involving single-ion anisotropies and Heisenberg terms with AFM J_1 and J_2' and FM J_2 , consistent with calculations [28] and with the values postulated here. The nearest-neighbor exchange J_1 is thought to be AFM in all known $\text{Ln}_2\text{O}_2\text{M}_2\text{OSe}_2$ materials and

dominates for $\text{La}_2\text{O}_2\text{Mn}_2\text{OSe}_2$ [27,30,41]. However, in the $2-k$ model, the J_1 interactions are unimportant as nearest-neighbor moments are perpendicular. Instead, it is the next-nearest neighbors J_2 and J_2' that dominate. DFT calculations predict that J_2 via Se^{2-} is FM for $M = \text{Fe}$, but AFM for $M = \text{Mn}$ and Co , while J_2' (180° exchange via O^{2-}) is predicted to be AFM for all M [42]. The FM J_2 Fe-Se-Fe interactions, predicted by DFT, are consistent with the FM chain structure reported for $\text{Ce}_2\text{O}_2\text{FeSe}_2$ [43]. 2D exchange concomitant with magnetocrystalline anisotropy (due to partially unquenched orbital angular momentum) is likely to stabilize the $2-k$ structure [and the $k = (\frac{1}{2} \frac{1}{2} 0)$ structure reported for $\text{La}_2\text{O}_2\text{Co}_2\text{OSe}_2$] [27,31]. This agrees with the Ising-like character suggested to constrain M^{2+} moments to lie along perpendicular local axes within the ab plane for $M = \text{Fe}$, Co (i.e., along Fe-O bonds in $\text{La}_2\text{O}_2\text{Fe}_2\text{OSe}_2$). This anisotropy is not found in the high-spin $M = \text{Mn}^{2+}$ for which orbital angular momentum is zero and moments are oriented out of the ab plane [27,30]. This anisotropy overrides J_1 and with FM J_2 and AFM J_2' , favors the $2-k$ over the collinear model.

To stabilize $2-k$ structures, energy terms beyond second-order isotropic or antisymmetric exchange (Dzyaloshinskii-Moriya) are required. Anisotropic exchange arising from spin anisotropy is able to introduce higher order terms that can stabilize combining the $2-k$ components. In doing so, the C_4 rotational symmetry that relates the two k vectors is reintroduced into the magnetic symmetry, constraining the moments of what were two independent orbits in the single- k structure, to be equal in magnitude and related in-phase. This constraint causes the magnetic ordering to satisfy entropic requirements and the transition is second order as observed here by experiment.

While the $2-k$ structure cannot be stabilized by second-order spin terms alone, it is useful to explore the structure in terms of the interactions in Fig. 1, which still embodies the two orbit structure of the single- k model. In it, with no net J_1 nearest-neighbor interactions, the $2-k$ model can be thought of as two interpenetrating square sublattices, each described by one of the two k vectors. Within each sublattice, J_2' coupling leads to AFM Fe-O-Fe stripes which are coupled by FM J_2 Fe-Se-Fe interactions. The $2-k$ model [and the $k = (\frac{1}{2} \frac{1}{2} 0)$ structure described for $\text{La}_2\text{O}_2\text{Co}_2\text{OSe}_2$] could result from dominant J_2' interactions where $J_2' \gg J_1, J_2$. This exchange scenario would lead to a network of perpendicular quasi-1D AFM Fe-O-Fe chains. However, our experimental results indicate 2D-like magnetic exchange interactions making this quasi-1D scenario unlikely.

The $2-k$ model can be compared with the magnetic ordering reported for Fe_{1+x}Te [44] which is also composed of two interpenetrating square sublattices [16,17]. First, the origin of the anisotropy within each sublattice in Fe_{1+x}Te (i.e., AFM interactions along a_T and FM interactions along b_T where the T subscript denotes tetragonal unit cell) is ascribed to orbital ordering, while in $\text{La}_2\text{O}_2\text{Fe}_2\text{OSe}_2$, the anisotropy within each single- k sublattice is due to different exchange

interactions along each direction. Second, the mechanism for coupling the two sublattices differs, with double-exchange interactions proposed for metallic Fe_{1+x}Te [45] being less likely for insulating $\text{La}_2\text{O}_2\text{Fe}_2\text{OSe}_2$. Rather, the strong spin-anisotropy observed supports a coupling by high-order anisotropic exchange terms.

The observation of a Warren peak characteristic of short-range magnetic ordering only ~ 14 K above T_N (in contrast to ~ 140 K above T_N for $\text{La}_2\text{O}_2\text{Mn}_2\text{OSe}_2$) [30] further supports the assignment of the (less frustrated) $2-k$ rather than the collinear model. This is because the $2-k$ structure diminishes the effects of J_1 and avoids frustration of J_2 and J_2' . With both J_2 and J_2' satisfied, the $2-k$ structure involves less frustration than in the Mn analogs. The anisotropic broadening of magnetic Bragg reflections suggests that there is only a small energy cost for disrupting the magnetic ordering along c (e.g., introducing stacking faults or antiphase boundaries) giving a reduced magnetic correlation length in this direction.

DFT calculations have supported the notion of large exchange constants in this material and related iron-based systems, in contrast with our experimental results. Given that J is proportional to $4t^2/U$ [46], these small J values determined experimentally suggest a small hopping integral t for these oxychalcogenides, consistent with theoretical work which describes band narrowing in these materials [14]. These small J values imply that local bonding is more important than in related materials such as Fe_{1+x}Te and $Ln\text{FeAsO}$, and that $\text{La}_2\text{O}_2\text{Fe}_2\text{OSe}_2$ is a more correlated system than current DFT work suggests.

The integrated intensity over the small bandwidth of excitations recovers the total moment for $S = 2$. While this is consistent with a large ordered moment, it implies that Fe^{2+} is in a weak crystal field favoring a Hund's rules population of the d orbitals, which contrasts with suggestions of an $S = 1$ ground state from analysis of pnictide and chalcogenide superconductors [45,47]. Our analysis, combined with the large ordered magnetic moments reported in $\text{K}_x\text{Fe}_{2-y}\text{Se}_2$, may indicate that the $S = 1$ parent state may need to be reconsidered.

In conclusion, Mott insulating $\text{La}_2\text{O}_2\text{Fe}_2\text{OSe}_2$ adopts a multicomponent $2-k$ magnetic structure. This structure is stabilized by AFM J_2' and FM J_2 interactions and the magnetocrystalline anisotropy of the Fe site and leads to 2D-Ising-like spin fluctuations around the critical point. Surprisingly, the magnetic exchange interactions are very small in comparison with related systems and also the Mott insulating cuprates and an integrated intensity analysis implies an $S = 2$ ground state. This may indicate additional localization in these $Ln_2\text{O}_2M_2\text{OSe}_2$ materials which has not yet been explored theoretically.

We acknowledge STFC, EPSRC (EP/J011533/1), RSE, and the NSF (DMR-0944772) for funding. We thank E. Suard (ILL), R. Stewart (ISIS), and M. Green for assistance.

[1] Y. Kamihara, T. Watanabe, M. Hirano, and H. Hosono, *J. Am. Chem. Soc.* **130**, 3296 (2008).

[2] S. Margadonna, Y. Takabayashi, Y. Ohishi, Y. Mizuguchi, Y. Takano, T. Kagayama, T. Nakagawa,

- M. Takata, and K. Prassides, *Phys. Rev. B* **80**, 064506 (2009).
- [3] C. de la Cruz, Q. Huang, J. W. Lynn, J. Li, W. Ratcliff, II, J. L. Zarestky, H. A. Mook, G. F. Chen, J. L. Luo, N. L. Wang, and P. Dai, *Nature (London)* **453**, 899 (2008).
- [4] P. A. Lee, N. Nagaosa, and X. G. Wen, *Rev. Mod. Phys.* **78**, 17 (2006).
- [5] I. I. Mazin, *Nature (London)* **464**, 183 (2010).
- [6] D. C. Johnston, *Adv. Phys.* **59**, 803 (2010).
- [7] J. Paglione and R. L. Greene, *Nat. Phys.* **6**, 645 (2010).
- [8] Q. M. Si, *Nat. Phys.* **5**, 629 (2009).
- [9] M. Qazilbabs, J. J. Hamlin, R. E. Baumbach, L. J. Zhang, D. J. Singh, M. B. Maple, and D. N. Basov, *Nat. Phys.* **5**, 647 (2009).
- [10] Z. P. Yin, K. Haule, and G. Kotliar, *Nat. Mater.* **10**, 932 (2011).
- [11] Q. M. Si and E. Abrahams, *Phys. Rev. Lett.* **101**, 076401 (2008).
- [12] F. Kruger, S. Kumar, J. Zaanen, and J. van den Brink, *Phys. Rev. B* **79**, 054504 (2009).
- [13] J. M. Mayer, L. F. Schneemeyer, T. Siegrist, J. V. Waszczak, and B. V. Dover, *Angew. Chem. Int. Ed. Engl.* **31**, 1645 (1992).
- [14] J. X. Zhu, R. Yu, H. Wang, L. L. Zhao, M. D. Jones, J. Dai, E. Abrahams, E. Morosan, M. Fang, and Q. Si, *Phys. Rev. Lett.* **104**, 216405 (2010).
- [15] D. G. Free and J. S. O. Evans, *Phys. Rev. B* **81**, 214433 (2010).
- [16] W. Bao, Y. Qiu, Q. Huang, M. A. Green, P. Zajdel, M. R. Fitzsimmons, M. Zhernenkov, S. Chang, M. Fang, B. Qian, E. K. Vehstedt, J. Yang, H. M. Pham, L. Spinu, and Z. Q. Mao, *Phys. Rev. Lett.* **102**, 247001 (2009).
- [17] E. E. Rodriguez, C. Stock, P. Zajdel, K. L. Krycka, C. F. Majkrzak, P. Zavalij, and M. A. Green, *Phys. Rev. B* **84**, 064403 (2011).
- [18] Y. Fuwa, M. Wakeshima, and Y. Hinatsu, *J. Phys. Condens. Matter* **22**, 346003 (2010).
- [19] R. Coldea, S. M. Hayden, G. Aeppli, T. G. Perring, C. D. Frost, T. E. Mason, S. W. Cheong, and Z. Fisk, *Phys. Rev. Lett.* **86**, 5377 (2001).
- [20] C. Stock, R. A. Cowley, W. J. L. Buyers, R. Coldea, C. L. Broholm, C. D. Frost, R. J. Birgeneau, R. Liang, D. Bonn, and W. N. Hardy, *Phys. Rev. B* **75**, 172510 (2007).
- [21] R. A. Ewings, T. G. Perring, R. I. Bewley, T. Guidi, M. J. Pitcher, D. R. Parker, S. J. Clarke, and A. T. Boothroyd, *Phys. Rev. B* **78**, 220501 (2008).
- [22] J. Zhao, D. T. Adroja, D. X. Yin, R. Bewley, S. Li, X. F. Wan, X. H. Chen, J. Hu, and P. Dai, *Nat. Phys.* **5**, 555 (2009).
- [23] S. O. Diallo, V. P. Antropov, T. G. Perring, C. Broholm, J. J. Pulikkotil, N. Ni, S. L. Budko, P. C. Canfield, A. Kreyssig, A. I. Goldman, and R. J. McQueeney, *Phys. Rev. Lett.* **102**, 187206 (2009).
- [24] O. J. Lipscombe, G. F. Chen, C. Fang, T. G. Perring, D. Abernathy, A. D. Christians, T. Egami, N. Wang, J. Hu, and P. Dai, *Rev. Rev. Lett.* **106**, 057004 (2011).
- [25] See Supplemental Material at <http://link.aps.org/supplemental/10.1103/PhysRevB.89.100402s> for details of synthesis, Rietveld refinements, fitting of Warren peak, candidate magnetic structures, sum rules, single-mode approximation, spin-wave analysis of INS data, and mean-field description of Curie-Weiss temperature.
- [26] B. E. Warren, *Phys. Rev.* **59**, 693 (1941).
- [27] D. G. Free, N. D. Withers, P. J. Hickey, and J. S. O. Evans, *Chem. Mater.* **23**, 1625 (2011).
- [28] L. L. Zhao, S. Wu, J. K. Wang, J. P. Hodges, C. Broholm, and E. Morosan, *Phys. Rev. B* **87**, 020406 (2013).
- [29] J. H. Her, P. W. Stephens, Y. Gao, G. L. Soloveichil, J. Rijssenbeek, M. Andrus, and J. C. Zhao, *Acta Cryst. B* **63**, 561 (2007).
- [30] N. Ni, E. Climent-Pascual, S. Jia, Q. Huang, and R. J. Cava, *Phys. Rev. B* **82**, 214419 (2010).
- [31] Y. Fuwa, T. Endo, M. Wakeshima, Y. Hinatsu, and K. Ohoyama, *J. Am. Chem. Soc.* **132**, 18020 (2010).
- [32] S. D. Wilson, C. R. Rotundu, Z. Yamani, P. N. Valdivia, B. Freelon, E. Bourret-Courchesne, and R. J. Birgeneau, *Phys. Rev. B* **81**, 014501 (2010).
- [33] N. Ni, S. Jia, Q. Huang, E. Climent-Pascual, and R. J. Cava, *Phys. Rev. B* **83**, 224403 (2011).
- [34] W. Bao, Q. Z. Huang, G. F. Chen, M. A. Green, D. M. Wang, J. B. He, and Y. M. Qiu, *Chin. Phys. Lett.* **28**, 086104 (2011).
- [35] J. Zhao, H. Cao, E. Bourret-Courchesne, D. H. Lee, and R. J. Birgeneau, *Phys. Rev. Lett.* **109**, 267003 (2012).
- [36] P. C. Hohenberg and W. F. Brinkman, *Phys. Rev. B* **10**, 128 (1974).
- [37] P. R. Hammar, D. H. Reich, C. Broholm, and F. Trouw, *Phys. Rev. B* **57**, 7846 (1998).
- [38] C. Stock, L. C. Chapon, O. Adamopoulos, A. Lappas, M. Giot, J. W. Taylor, M. A. Green, C. M. Brown, and P. G. Radaelli, *Phys. Rev. Lett.* **103**, 077202 (2009).
- [39] B. J. Campbell, H. T. Stokes, D. E. Tanner, and D. M. Hatch, *J. Appl. Cryst.* **39**, 607 (2006).
- [40] A. S. Wills, *Physica B* **276–278**, 680 (2000).
- [41] H. J. Koo and M. H. Whangbo, *J. Magn. Magn. Mater.* **324**, 3859 (2012).
- [42] J. B. Goodenough, *Magnetism and the Chemical Bond* (John Wiley and Sons, Inc., New York, 1963).
- [43] E. E. McCabe, D. G. Free, and J. S. O. Evans, *Chem. Commun.* **47**, 1261 (2011).
- [44] S. Li, C. Cruz, Q. Huang, Y. Chen, J. W. Lynn, J. Hu, Y. L. Huang, F. C. Hsu, K. W. Yeh, M. K. Wu, and P. Dai, *Rev. Rev. B* **79**, 054503 (2009).
- [45] A. M. Turner, F. Wang, and A. Vishwanath, *Phys. Rev. B* **80**, 224504 (2009).
- [46] A. H. MacDonald, S. M. Girvin, and D. Yoshioka, *Phys. Rev. B* **37**, 9753 (1988).
- [47] K. Haule and G. Kotliar, *New J. Phys.* **11**, 025021 (2009).